# Fitting by Orthonormal Polynomials of Silver Nanoparticles Spectroscopic Data

Nina B. Bogdanova (Email:nibogd@inrne.bas.bg)
*INRNE,BAS,72 Tzarigradsko choussee,1784 Sofia, Bulgaria*
*LIT,JINR* (Email:bogd@jinr.ru)
and
Mihaela E. Koleva (Email:Mihaela_ek@yahoo.com)
*IE,BAS,72 Tzarigradsko choussee,1784 Sofia, Bulgaria*

Our original Orthonormal Polynomial Expansion Method (OPEM) [1] in one-dimensional version is applied for first time to describe the silver nanoparticles spectroscopic data. The experimental errors in variables shown by experimentalists are included in weights for approximation - different in every point. In this way we construct orthogonal (orthonormal ) polynomials for presenting the curve. The corridors of given data by the help of the weights define the optimal behavior of searched curve. We have received four curves in thousands points for analysis. We have chosen one subinterval in one of them.

This study describes the $Ag$ nanoparticles produced by laser approach in a $ZnO$ medium forming a $AgNPs/ZnO$ nanocomposite heterostructure. The most important subinterval of spectra data is investigated, where the minimum (Surface Plasmon resonance absorption) is looking for. We hope that with our description we target the experimental work in regular direction.

# CONTENT

# 1. INTRODUCTION

The metal nanostructures have attracted considerable attention due to their optical properties. It is related to the efficient excitation of collective electron oscillations, plasmons, which define the particle response to external electromagnetic field. The resonant frequency of these oscillations usually falls in deep UV spectral region. For some metals, as silver, the plasmon resonance is realized in the near UV or visible spectral range. This makes these metals good candidates for resonance plasmon excitation sources and for utilizing their properties in the region where commercially available coherent lights sources work [2]. The efficient plasmon excitation shows a drastic enhancement of heir extinction coefficients. These unique properties of metal nanoparticles are used in development of different techniques and systems for applications in optical, electronic, catalytic, sensing and biomedical devices [4, 5, 6].

Back
Close

# Fig. 1: **Experimental curves**

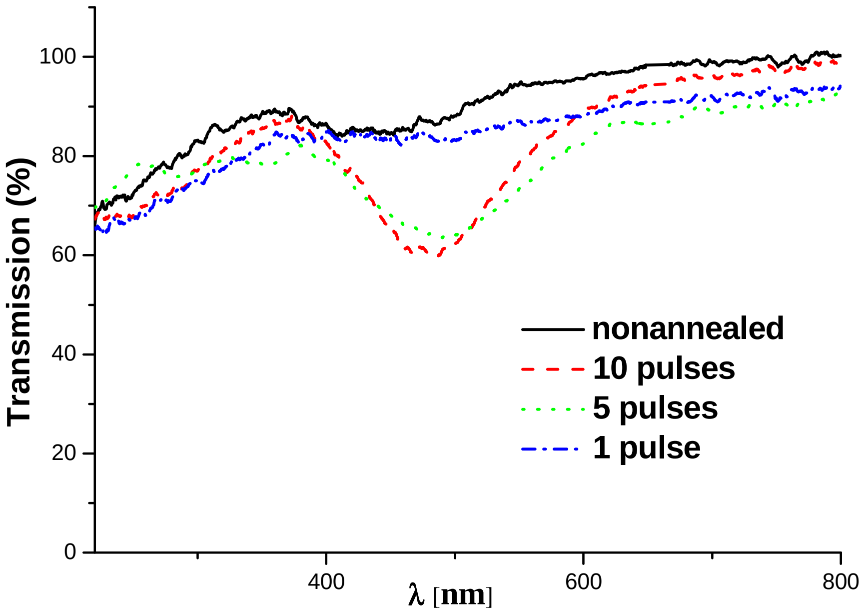



Back
Close

Fig. 2: **SEM images of Ag/ZnO after and before nanostructuring**

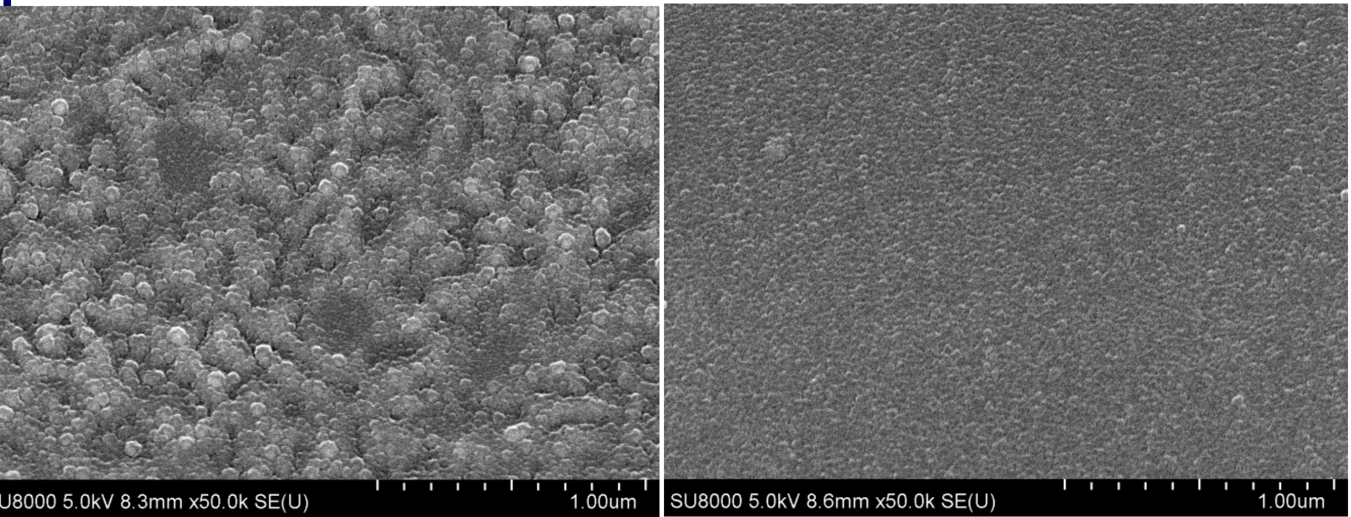

The laser annealing leads to decomposition of the layer into nanoparticles by dewetting mechanism [3]. The evolution of the dewetting process is a function of the thin film composition and dictates the size distribution and spacing of the nanoparticles.

The practical applications and the properties of nanostructures of noble metals are strictly related to the material in which they are embedded, and a number of studies focus on developing methods for preparing composite materials containing nanoparticles. The NPs incorporation into dielectric or semiconductor matrices can lead to the emergence of new features with composite materials showing properties different from those of the individual components [6, 7, 8, 9]. The application of methods for precise study of the resonance absorption band position and shifting of noble metal nanoparticles is of particular interest.

## 2. PHYSICAL DATA

**The silver nanoparticles are produced by pulsed laser deposition (PLD) on quartz substrates SiO2 (001) in a vacuum chamber. The films are deposited by a Nd:YAG ( 355 nm, =18 ns, =10 Hz) at laser fluence of F = 1.5 J/cm2 at room temperature. The films are post-deposition annealed for surface nanostructuring by laser-induced decomposition of the film into nanoparticles with diameters in the range of  few tens of nanometers. The deposited films are laser annealed in air by the same laser system with a fluence of 200 mJ/cm2. The transmission spectrum of the Ag nanoparticles was analyzed using a UV-VIS spectrometer (HR 4000 Ocean optics) in the range of 220 - 800 nm.**

**We have chosen one subinterval in one of them with $M = 94$ points and $\lambda$ in [468.9,493.2]. The selected curve corresponds to the transmission spectrum of AgNPs after the annealing by 10 laser pulses. The lower number of pulses smaller than 5 leads to incomplete decomposition of the layer into nanoparticles. The laser annealing is performed at different number of laser pulses (1, 5 and 10) but at the same laser fluence. For more detailed approximation( for test) we have taken the smaller interval with $M = 50$ points in the above one with $\lambda$ in $[468.9, 481.7]$.**

# 3. MOTIVATION AND PROBLEM DEFINITION

- **To find the best approximation curve $T^{appr}$ of measured data $T$ on Fig 1, including errors in variables;**
- **To extend our original Orthonormal polynomial expansion method (OPEM), according some criteria, to evaluate orthonormal description of given data.**

# 4.Mathematical approach

**Here one defines new variance at** $i-th$ **given point** $(\lambda_i, T_i), i = 1, 2, ...M$**, following [11] Bevington** [1] **and [12] G. Jones** [2]**, using expression**

$$S_i^2 = {\sigma_{T_i}}^2 + (\frac{\partial T_i}{\partial \lambda_i})^2 {\sigma_{\lambda_i}}^2. \quad (1)$$

**In the formula (1) the Bevington's (1969) [11] proposal to combine both variable uncertainties and assign them to dependent variable is used. The so called method is OPEM total(effective) variance method.**

[1] P. R. Bevington, *Data Reduction and Error Analysis for the Physical Sciences* (McGrow-Hill, New York, 1969).

[2] G. Jones, *Least Square Fitting when Both Variables have Errors*, Preprint TRI-PP-92-31 A, 1992

## The generalized OPEM

**Our principal relation for one-dimensional generation of orthonormal polynomials by Forsythe [13] [3] $\{P_i^{(0)}, i = 1, 2, \ldots\}$ and their derivatives $\{P_i^{(m)}, m = 1, 2, \ldots\}$, in arbitrary discrete point set in OPEM is:**

$$P_{i+1}^{(m)}(E) = 1/\nu_{i+1}[(T-\mu_{i+1})P_i^{(m)}(\lambda)-(1-\delta_{i0})\nu_i P_{i-1}^{(m)}(\lambda)+mP_i^{(m-1)}(\lambda)]. \quad (2)$$

**The generalization of Forsythe procedure in one-dimensional case is with involving arbitrary weights in every points, evaluating derivatives ($m > 0$) or integrals ( $m < 0$) and normalizing polynomials. Here the normalization coefficient $1/\nu_i$ and the recurrence coefficients $\mu_i, \nu_i$ are given as scalar products of the polynomials in the given data in $M$ points [14][4] in our earlier paper. We developed some features of our algorithm. One can generate $P_i^{(m)}(\lambda)$ recursively. The polynomials satisfy the following orthonor-**

[3] G. Forsythe, J. Soc.Ind. Appl. Math. **5**, 74 (1957).
[4] V.Gadjokov, N. Bogdanova, Commun.JINR, P11-12860, 1979.

**mality relations**

$$\sum_{i=1}^{M} w_i P_k^{(0)}(\lambda_i) P_l^{(0)}(\lambda_i) = \delta_{k,l}$$

**over the discrete point set** $\{\lambda_i, i = 1, 2, \ldots\}$ **where** $w_i = 1/(\sigma_{T_i}^2)$ **are the corresponding weights. The coefficient matrix in the least square method becomes an identity matrix and due to orthogonality conditions the coefficients** $a_k$ **in**

$$T^{appr\,(m)}(\lambda) = \sum_{k=0}^{L} a_k P_k^{(m)}(\lambda) \tag{3}$$

**are easily computed by**

$$a_k = \sum_{i=1}^{M} T_i w_i P_k^{(m)}(\lambda_i). \tag{4}$$

**The approximation function** $T^{ap}$ **is constructed as follows with orthonormal** $a_k$ **and usual coefficients** $c_k$**:**

**The inherited errors in usual coefficients are given by the inherited errors in orthonormal coefficients:**

$$\Delta c_j = (\sum_{i=j}^{L} (c_j^{(i)})^2)^{1/2} \Delta a_i, j = 0, 1, 2..., L \tag{5}$$

**And the inherited errors in orthonormal coefficients are expressed by:**

$$\Delta a_i = [\sum_{k=1}^{M} P_i^2(\lambda_k) w_k (T_k - T_k^{\mathrm{appr}})^2]^{1/2}, i = 0, ..., L. \tag{6}$$

**It is worth noting the following advantages of OPEM: a) It avoids recomputing the coefficients in eq.(6)- for evaluating approximation with higher degree polynomials we use unchanged the coefficients of the lower-order polynomials. b) it avoids the procedure of inversion of the coefficient matrix to obtain the solution and this shortens the computing time. For appropriate classes of examples this diminishes the number of iterations required to reach a prescribed numerical precision.**

**The development now is carried out to decide the approximation task with errors in variables. Two criteria are used here to select the optimum series length in equation (3).**

**First criterion** **(i) Here one neglects the errors in $\lambda$ variable, the graph of the fitting curve lies inside the "old" error corridor $[T-\sigma, T+\sigma]$.**
**(ii) After calculating the derivatives at any point $\lambda_i$ using equations (1),(2),(3),(4) the fitting curve has to lie inside the total error corridor $[T-S, T+S]$.**

**Second criterion** **We extend the above algorithm to include $S_i^2$ in OPEM in two stages:**
**(i). i.e. the following $\chi^2$ is minimized**

$$\chi^2 = \sum_{i=1}^{M} w_i [T^{ap}(\lambda_i) - T(\lambda_i)]^2 / (M - L - 1),$$

**where the weights are $w_i = 1/\sigma_{T_i}^2$.**

Back
Close

**(ii): The next approximation is calculated with the weight function $w_i = 1/S_i^2$.**

**The results of calculations in (i) gives the first approximation. The procedure is iterative and the result of the consequent $k^{it}$-th iteration, $k^{it} > 1$, is called below the $k^{it}$-th approximation. The preference is given to the first criterion and when it is satisfied, the search for the minimal chi-squared stops. Based on the above features the algorithm selects the optimal solution for a given set $\{T, \lambda\}$.**

**Criterion for usual expansion** After evaluating an optimal number of polynomials in orthonormal expansion we find the best result of usual expansion for every step of iteration by minimization of:

$$max|T_a^{appr} - T_c^{appr}| = max_{i=1}^{M}|T_a^{appr}(\lambda_i) - T_c^{appr}(\lambda_i)|$$

**Now the algorithm is called total (effective) OPEM [15, 16, 17, 18, 19, 20].**

# 5. Approximation results

- **A. Mathematical analysis**

  **The main approximation results are given in Table 1. and Figures. We have used one subinterval with $M = 94$ points around supposed minimum of $T$ and other subinterval with $M = 50$ points in it. Here we present the approximation with orthonormal coefficients. We tried to use 2 different type of weights. The table shows the results with : number of points M, optimal number of degrees of polynomials $L$, $\sqrt{\chi^2}$, maximal deviation between given and approximated values $max|T^{appr} - T|$, $\lambda$[nm] at $max|T^{appr} - T|$, and the most interesting results: $T_{min}$ and the corresponding $\lambda(T_{min})$. The best results are in bigger subinterval**

  - **in second row with $T_{min}^{appr} = 60.32$ and $\sqrt{\chi^2} = 0.23$ in 481 nm (54-th point) at $L = 2$ number of degrees (fig. 4).**

Back
Close

– **and third row with** $T_{min}^{appr} = 59.85$ **and** $\sqrt{\chi^2} = 0.24$ **in 485 nm ( 65-th point) at** $L = 3$ **number of degrees (fig. 3).**

Table 1: **OPEM approximations results for different given subintervals**

| $M$ | L | $\sqrt{\chi^2}$ | W | $max\|T^{ap}-T\|$ | $\lambda(\max\|T^{ap}-T\|)$ | $T^{ap}_{min}$ | $\lambda(T^{ap}_{min})$ |
|---|---|---|---|---|---|---|---|
| 50 | 2 | 0.12 | $10^3/T^2$ | 0.57 | 481. | 59.67 | 473. |
| 94 | 2 | 0.23 | $10^3/T^2$ | 0.84 | 474. | 60.32 | 481. |
| 94 | 3 | 0.24 | 1. | 0.73 | 493. | 59.85 | 485. |

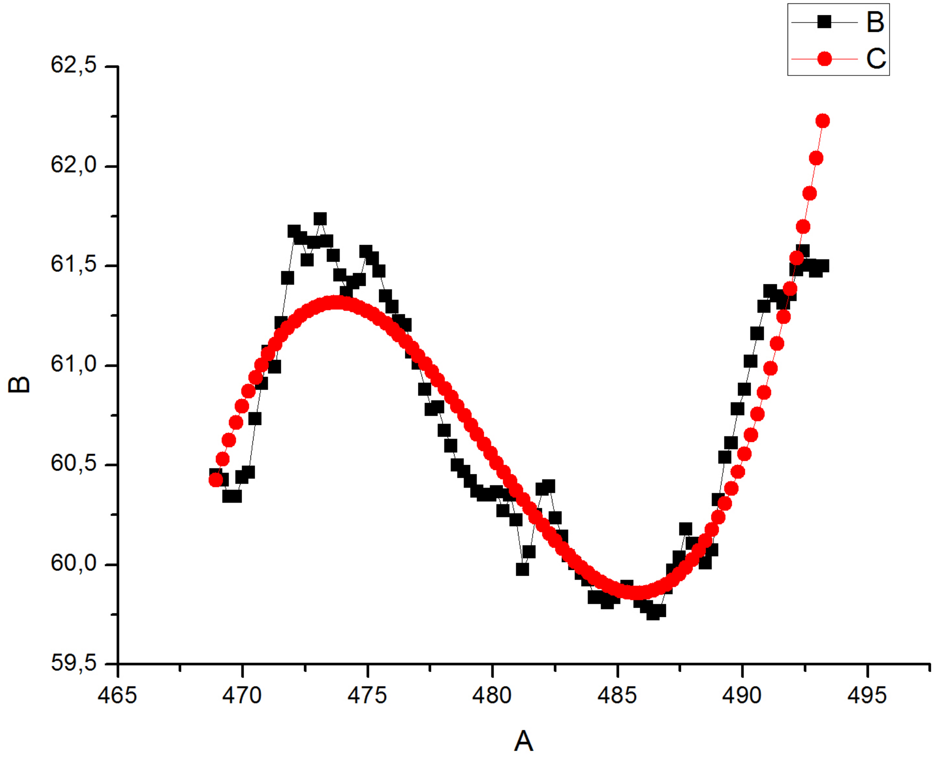


Fig. 3: Experimental data $T$ (black) and OPEM approximated $T^{appr}$ (red) by equal weghts and $L = 3$

]

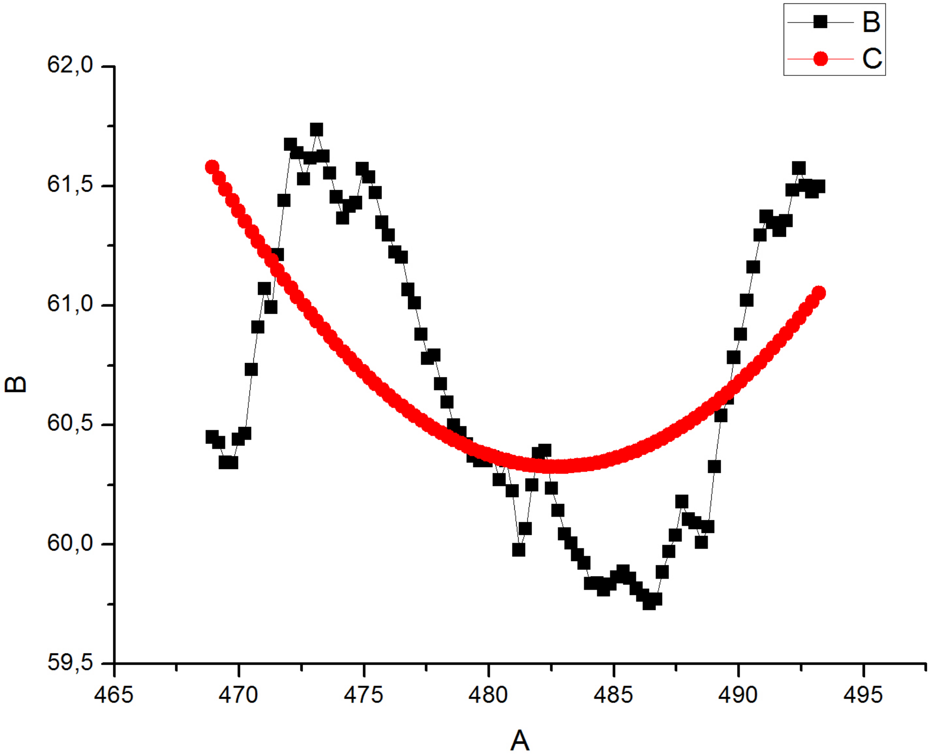


Fig. 4: Experimental data $T$(black) and OPEM approximated $T^{appr}$ (red) and $L = 2$

Back
Close

- B.Physical analysis
  The nanostructured samples exhibit clearly pronounced surface plasmon absorption. The transmission spectrum on Fig. 1 exhibits a minimum at about 490 nm. The Ag nanoparticles with a mean size of 30 nm and size distribution in the range of (15-75) are described in this work. The optical properties of AgNPs in ZnO environment are studied. The PLD grown thin film is transformed to a discontinuous structure consisted of small particles at certain laser fluence. These transformations are governed by seeds coming from the grains boundaries of the polycrystalline thin film. The small metal islands become in liquid phase with increasing of the incident energy. The shape of the formed particles at this stage is quasi-spherical. The laser annealing with different number of laser pulses, reveals the activation of different mechanisms, as the thermal behavior and structure variation of the nanostructures differ from conventional thermal annealing treatments and can be controlled by the laser parameters. An unusual island motion has been observed under the action of subsequent laser pulses (5). The morphology of the samples annealed at 1 laser pulse show the same morphology as the as-grown films.

Back
Close

The layers morphology changes significantly with the number of laser pulses. The shape of the formed particles at 10 laser pulses is quasi-spherical. The laser annealing of layers in ZnO medium shifts the absorption band towards longer wavelengths (red-shift) with respect to the as-grown films and to the air surrounded medium. Changes in resonance absorption are usually associated with changes in size, shape and interparticle distances, as well as with the dielectric constant of the surrounded medium [4-10].

# 6.Main Conclusions

- The all main results given in table and figures show smooth approximation with second and third number of degrees of polynomials.
- The results, given in table 1 and figures 3. and 4., show the $T_{min}^{appr}$ is in $\lambda = 481.nm$ and $\lambda = 485.nm$ ( 54-th and 65-th numbers of points ) respectively by two approaches.
- The present version of total OPEM approximation gives good results for further interpretations and comparisons in laser produced nanoparticles .

# References


[1] N. Bogdanova, J. Comp. Appl. Mathem. 1986. **14**, 345.

[2] Q. Zhang, Y.N. Tan, J. Xie, J.Y. Lee, Colloidal Synthesis of Plasmonic Metallic Nanoparticles Plasmonics 4 (2009)

[3] Henley, S. J., Carey, J. D. and Silva, S. R. P., Pulsed-laser-induced nanoscale island formation in thin metalon-oxide films, Phys. Rev. B 72, 195408 (2005).

[4] M.E. Koleva, A.Og. Dikovska, N.N. Nedyalkov, P.A. Atanasov, I. Bliznakova, Enhancement of ZnO photoluminescence by laser nanostructuring of Ag underlayer, Applied Surface Science, 258/23, (2012) 9181-9185.

[5] M. Koleva, N. N. Nedyalkov, P. A. Atanasov, J. W. Gerlach, D. Hirsch, A. Prager, B. Rauschenbach, N. Fukata, W. Jevasuwan Porous plasmonic nanocomposites for SERS substrates fabricated by two-step laser method J. Alloy. Compd. 665 (2016) 282-287.

[6] Koleva M.E., Nedyalkov N.N., Fukata N., Jevasuwan W., Amoruso, S., Laser nanostructuring for plasmon enhancement of Ag/ZnO optical characteristics, 2017, Proceedings of SPIE - The International Society for Optical Engineering, 10226, 1022609.

[7] M. E. Koleva, N. N. Nedyalkov, P. A. Atanasov, N. Fukata, M. Dutta, Optical properties of Ag-ZnO nanostructures, Proc. of SPIE Vol. 9447 94470E-1, 2015.

[8] Koleva M.E., Nedyalkov N.N., Atanasov P.A, Effect of the plasmon-exciton coupling on the optical response of a ZnO/Ag/ZnO nanocomposites, Journal of Physics, Vol. 514, Issue 1, Article number 012031, 2014.

[9] Koleva M.E., Nedyalkov N.N., Dikovska A.O., Atanasov P.A., Avdeev G.V., Shimizu H., Terakawa M., Obara M., Pallotti D., Orabona E., Maddalena P., Lettieri S., Nanostructured Ag/ZnO multilayer plasmonic composites, Journal of Optoelectronics and Advanced Materials, Vol. 16, Issue 1-2, 144-148, 2014.

[10] Koleva M.E., Dikovska A.Og., Nedyalkov N.N., Atanasov P.A., Atanasova G.B., Ag/ZnO nanocomposites prepared by laser meth-

ods, Proc. of SPIE, 8770, art. no. 877007, 2013.

[11] P. R. Bevington, *Data Reduction and Error Analysis for the Physical Sciences* (McGrow-Hill, New York, 1969).

[12] G. Jones, *Least Square Fitting when Both Variables have Errors*, Preprint TRI-PP-92-31 A, 1992.

[13] G. Forsythe, J. Soc.Ind. Appl. Math. **5**, 74 (1957).

[14] V.Gadjokov, N. Bogdanova, Commun.JINR, P11-12860, 1979(in Russian).

[15] N.Bogdanova, Commun. JINR, Dubna, E11-98-3,1998.

[16] N.Bogdanova, St.Todorov, IJMPC **12** (2001 )pp. 117-127.

[17] N. Bogdanova, reported at BPU6 Conf., Istanbul, August 2006, in 2007 AIP proceedings, edited by S.A.Cetin , I.Hikmet, 978-0-735400404-5/07, p. 377.

[18] N.Bogdanova, S. Todorov, Bulletin of PFUR, ser. Mathematics,Information,Physics, (2010) No. 3(2),pp. 63-67.

[19] N. Bogdanova, S. Todorov, in MMCP2013 proceedings, Letters in PEPAN, 2015, v.12, 3, pp.608-613.

[20] N. Bogdanova, St. Todorov and G. A. Ososkov, Use of Orthonormal polynomial expansion method to the description of the energy spektra of biological liquids,E10-2015-67, Communication JINR. 2015.

# Thank you for your attention!